Journal of Alloys and Compounds 509 (2011) 2936–2941

Contents lists available at ScienceDirect

Journal of Alloys and Compounds

journal homepage: www.elsevier.com/locate/jallcom

Synthesis of $(Bi_{0.5}Na_{0.5})TiO_3$ (BNT) and Pr doped BNT using the soft combustion technique and its properties

Khairunisak Abdul Razak*, Chiah Jun Yip, Srimala Sreekantan

School of Materials and Mineral Resources Engineering, Engineering Campus, Universiti Sains Malaysia, 14300 Nibong Tebal, Penang, Malaysia

ARTICLE INFO

Article history:
Received 28 September 2010
Received in revised form
11 November 2010
Accepted 19 November 2010
Available online 30 November 2010

Keywords:
Chemical synthesis
Ceramics
Dielectric response
Microstructure

ABSTRACT

In this work, bismuth sodium titanate $(Bi_{0.5}Na_{0.5})TiO_3$ (BNT) and praseodymium (Pr)-doped BNT were successfully produced using the soft combustion technique. The effects of Pr doping on stoichiometry, microstructure, density and dielectric properties were studied. Pure Pr-doped BNT was obtained in all samples containing 5, 10 and 20 mol% Pr after calcination at 800 °C for 3 h. The produced powders were then pressed into pellets and sintered at 1100 °C for 3 h. The very similar ionic radii of Pr^{3+} with Bi^{3+} and Na^+ made it possible to substitute both Bi and Na. The crystallite size and grain size decreased with increasing Pr amount because Pr acted as grain growth inhibitor, both for calcined powders and for sintered pellets. Maximum density was obtained in 5 mol% Pr-doped BNT, beyond which density decreased. The maximum dielectric constant of 756 was obtained in 5 mol% Pr-doped BNT and decreased at higher levels of Pr doping. Pr doped into BNT also caused a decrease in dielectric loss.

1. Introduction

Piezoelectric ceramics are important in many electronic applications due to their unique properties. Their ability to convert mechanical stress to electrical output and vice versa makes them attractive for use in electronic and mechanical devices such as capacitors, sensors, and ultrasonic detectors. However, most current piezoelectric ceramics are lead-based (e.g. PZT, PLZT), making them environmentally unfriendly and hazardous to health. Moreover, volatilization of the lead components at temperatures as low as 800 °C also causes degradation of their dielectric properties [1–3]. In order to overcome these problems, research widely seeks candidates for lead-free piezoelectric ceramics.

$Bi_{0.5}Na_{0.5}TiO_3$ (BNT) is a promising perovskite-structure lead-free piezoelectric material. This compound has a large remnant polarization of 38 μC/cm^2 with a coercive field (E_c) of 73 kV/cm at room temperature. It also has a high Curie temperature of 320 °C [4]. However, a pure BNT system has many problems. Sintered pure BNT shows significant grain growth as well as non-uniform grain size distribution and shape. The large coercive field of pure BNT causes difficulty during poling [5–7]. Furthermore, some researchers have found that the piezoelectric properties of a pure BNT system are not very good. The surface of BNT often becomes conductive, causing high loss. BNT also has been widely studied with the addition of K, $BiNa_xK_{1-x}TiO_3$ (BNKT) as piezoelectric material because this compound has better dielectric properties than BNT alone [8,9]. However, the electrical properties are still not comparable to those of Pb-based piezoelectrics.

Therefore, research pursues its search for a suitable dopant for BNT that would enhance its desirable properties. Dopant segregated cation vacancies as well as acceptor solutes at the grain boundaries are used to induce the space-charge region [7], thereby inhibiting grain growth. In addition, some electrical properties such as dielectric properties, piezoelectric coefficient, and loss tangent can be enhanced by tuning the concentration of dopant. Very little information on the effects of dopants on BNT exists. However, the considerable research that has been carried out on doping of other lead-free compounds can provide useful guidance. CuO, MnO, MnO_2 and ZnO have been doped into piezoelectric compounds to reduce sintering temperature and improve electrical properties of the compounds [1,2]. CuO doping has proven beneficial to improve densification of the product [2]. Mn doping in BNT has been found to decrease phase transition temperature and to increase the values of electromechanical coupling factors and the piezoelectric constant d_{33}.

Doping of some rare earth elements in lead-free piezoelectrics has also been studied. Nd_2O_3-doped 0.82BNT–0.18BKT showed an improved piezoelectric constant [10]. Doping of 0.3 wt.% Sm_2O_3 in $0.82Bi_{0.5}Na_{0.5}TiO_3$–$0.18Bi_{0.5}K_{0.5}TiO_3$ exhibited the optimum properties with high piezoelectric constant (d_{33} = 147 pC/N) and high planar coupling factor (k_p = 22.4%) [11]. Doping of rare earth elements in $(Na_{0.5}Bi_{0.5})_{0.93}Ba_{0.07}TiO_3$ resulted in an increase in diffuseness in phase transition and a decrease in depolarization temperature (T_d). The doping of La_2O_3 or Pr_2O_3 resulted in electrical

* Corresponding author. Tel.: +60 4 5996126; fax: +60 4 5941011.
E-mail address: khairunisak@eng.usm.my (K.A. Razak).

0925-8388/$ – see front matter © 2010 Elsevier B.V. All rights reserved.
doi:10.1016/j.jallcom.2010.11.163

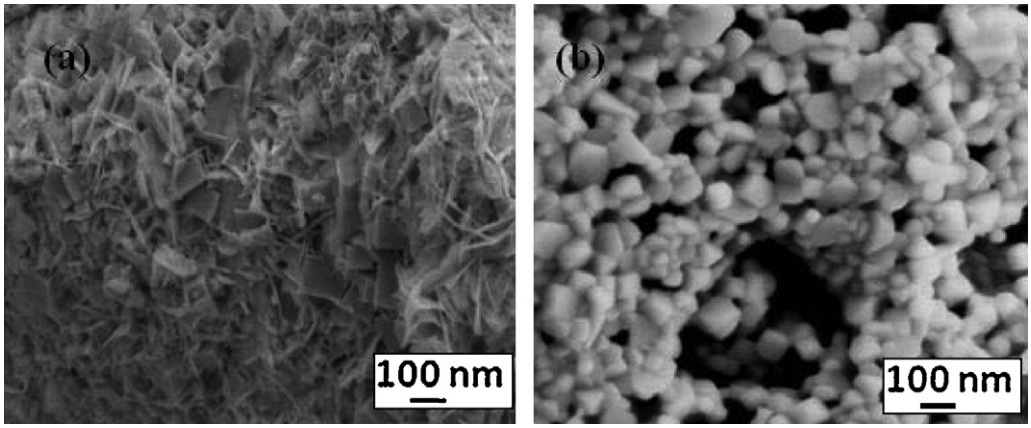

Fig. 1. SEM micrographs of BNT (a) as synthesized powders and (b) after calcination at 800 °C for 3 h.

properties following a soft doping effect. On the other hand, doping with Eu_2O_3 or Gd_2O_3 led to an abnormal change in the electrical properties, which was qualitatively interpreted as an internal stress effect [3]. Previous work has shown that Pr doping was beneficial in improving the dielectric properties of BIT [12].

BNT ceramic powder can be synthesized using a number of methods such as the solid state technique, the sol–gel technique, and the hydrothermal method [8,9,13–15]. The solid state method is limited by its requirement for a high sintering temperature (>1400 °C), causing Bi ion volatilization, which occurs at temperatures above 1130 °C [15]. Moreover, the solid state technique produces a powder with large particle size and a wide range particle size distribution. The sol–gel technique has been widely used to produce nanoparticles. However, the technique requires a long processing period and repeated heat treatment to obtain the desired products. The hydrothermal technique has the advantage of producing fine particle size. However, the stoichiometry of the products is dependent on the kinetics and thermodynamics of the elements during hydrothermal reaction. The soft combustion technique, in contrast, has the advantages of lower formation temperature, better homogeneity, a simple experimental set-up, relative inexpensiveness and production of fine size powders with a narrow particle size distribution range [12,16].

This work focused on the properties of BNT and praseodymium (Pr)-doped BNT synthesized using the soft combustion technique. BNT, a lead-free piezoelectric ceramic, was chosen for its environmental friendliness. The use of Pr as dopant was expected to improve the dielectric constant and reduce the grain size. Moreover, doping BNT with Pr was expected to result in homogenous grain growth and a narrower grain size distribution and shape. The soft combustion technique was selected for its low synthesis temperature, which minimizes volatilization of Bi.

2. Experimental details

BNT powder was prepared using the soft combustion technique. Bismuth nitrate and sodium nitrate were mixed and dissolved at 40 °C in 2-methoxyethanol. For Pr-doped BNT synthesis, praseodymium nitrate (5, 10, or 20 mol%) was mixed with bismuth nitrate and sodium nitrate. 1 mol of glycine was added into the solution to aid the combustion process. In parallel, 1 mol of titanium isopropoxide was dissolved separately in 2-methoxyethanol and acetylacetone. The acetylacetone functions as a chelating agent in the reaction. Next, the prepared titanium solution was continuously stirred into the prepared bismuth and sodium solution or Pr-doped bismuth sodium solution for 2 h, producing a yellowish homogeneous solution. The mixture was then heated to 130 °C on a hot plate with continuous stirring. Evaporation transformed the mixture into a viscous brownish solution. Continued heating at 130 °C led to combustion and the formation of foam. Next, the foam was ground using an agate mortar to form fine powder. The resulting powder was calcined at 800 °C for 3 h. The calcined powder was then pressed into pellets using 52.2 bar of pressure. The pellets were then sintered at 1100 °C for 3 h at a heating rate of 5 °C/min.

The microstructure of the samples was observed using scanning electron microscopy (FESEM; Zeiss SUPRA 35). Phase presence and stoichiometry of the samples were analyzed using X-ray diffractometer (XRD; Bruker AXS D8 Advance). Density of the samples was measured using Archimedes' method. For measurement of dielectric properties, silver paste was applied on both major surfaces of the sintered pellet, and capacitance and dielectric constant were measured using LCR meter (Agilent HP4284).

3. Results and discussion

In this work, $(Bi_{0.5}Na_{0.5})TiO_3$ (BNT) and Pr-doped BNT were produced using the soft combustion technique. Fig. 1(a) shows the SEM

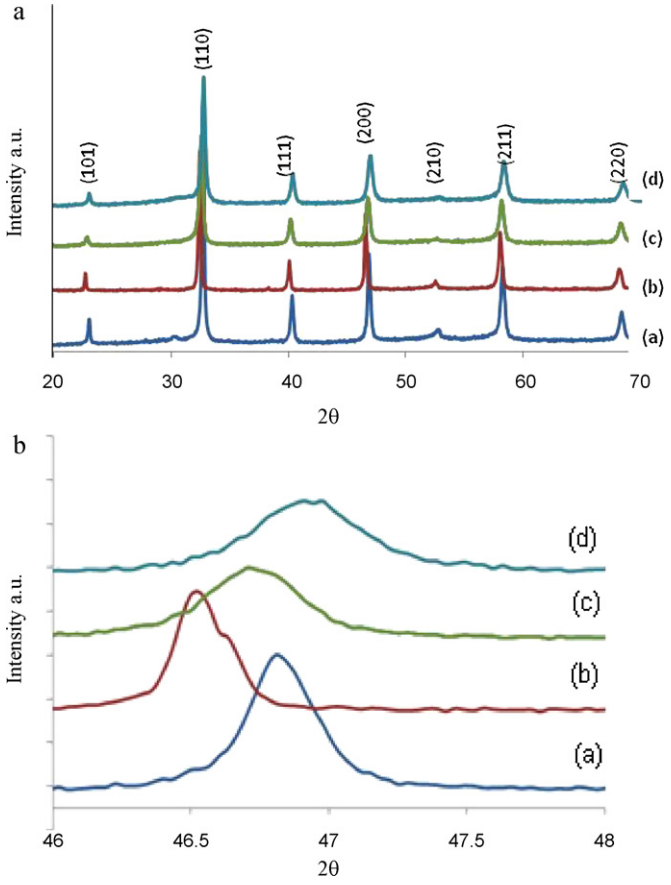

Fig. 2. XRD spectra of samples after calcination at 800 °C of (a) BNT, (b) 5 mol% Pr-doped BNT, (c) 10 mol% Pr-doped BNT and (d) 20 mol% Pr-doped BNT. [a] Wide scan XRD spectra and [b] XRD spectra of (2 0 0) peak position.

micrograph of BNT powder before calcination, showing the plate-like and pin-shaped BNT particles, indicating the lack of mutual solubility between the bismuth layer structure phase and the perovskite phase. The plate-like particles are the bismuth-layered phase whereas the smaller cubic or round particles with a size of 100 nm are regarded as perovskite. In Fig. 1(b), the SEM micrograph of BNT powder after calcination shows a distribution of nearly cubical or round particles. No plate-like particles appeared after calcination, indicating that calcination process fully transformed all bismuth layered phase into perovskite structure. A similar phenomenon was observed by Ma et al. [17]. They found that during the calcination process, some unwanted compounds such as water and carbon phases decomposed. At the same time, diffusion of ions occurred that led to the formation of pure compound with stable crystal structure. In this study, ions in the unstable bismuth-layered phase diffused and formed a more stable cubic or round particle with perovskite structure. The average particle size was around 140 nm.

The XRD spectra of BNT and BNT doped with varying amounts of Pr calcined in air at 800 °C for 3 h are shown in Fig. 2. A single perovskite phase was obtained for all Pr-doped BNT (JCPDS No. 36-340). At room temperature, pure BNT and Pr-doped BNT powders have rhombohedral symmetry. However, in the XRD spectra, rhombohedral structure is hard to distinguish due to the overlapping of peaks that could be due to nearly cubic lattice parameters. Although the crystal structure of BNT was rhombohedral, the diffraction lines were indexed based on the pseudocubic unit cell because of the small degree of rhombohedral distortion [18]. In BNT compound, the ionic radius of Bi is close to Na (1.03 Å and 1.02 Å, respectively), which causes a slight distortion of lattices [19]. Doping with Pr with ionic radius 1.013 Å in BNT caused a local lattice contraction that further distorts the lattices. However, since the ionic radii of those ions are very close, the changes in degree of lattice distortion are not obvious.

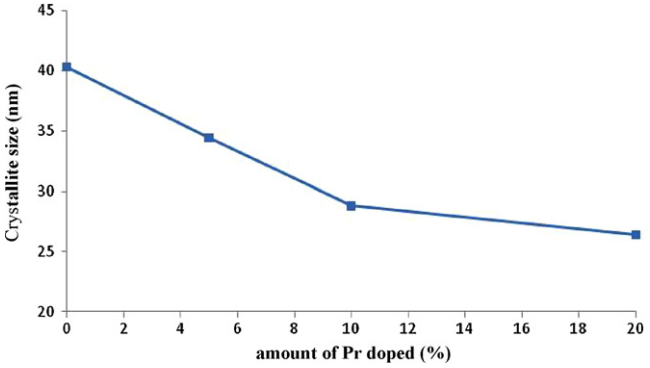

Fig. 3. Crystallite size of BNT doped with various levels of Pr after calcination at 800 °C for 3 h.

XRD spectra of Pr-doped BNT powders in Fig. 2[a] did not show any peak belonging to praseodymium oxide, which is taken to indicate the substitution of praseodymium ions into the perovskite lattice. The closeness of the ionic radii of the three elements enabled the ready substitution of Pr^{3+} ions for Bi^{3+} ions or Na^{+} ions into the perovskite lattice. Since the charge of Pr ions can be 2+ or 3+, Pr ions can substitute into the A-site in the BNT perovskite structure [7].

The XRD spectra of calcined BNT and Pr-doped BNT powders at the peak position (2 0 0) are shown in Fig. 2[b]. The peak position shift to the left was proportional to the level of Pr added. The result shows the change in the unit cell size that is caused by lattice distortion of BNT [4,19]. Some micro-strain occurred with the

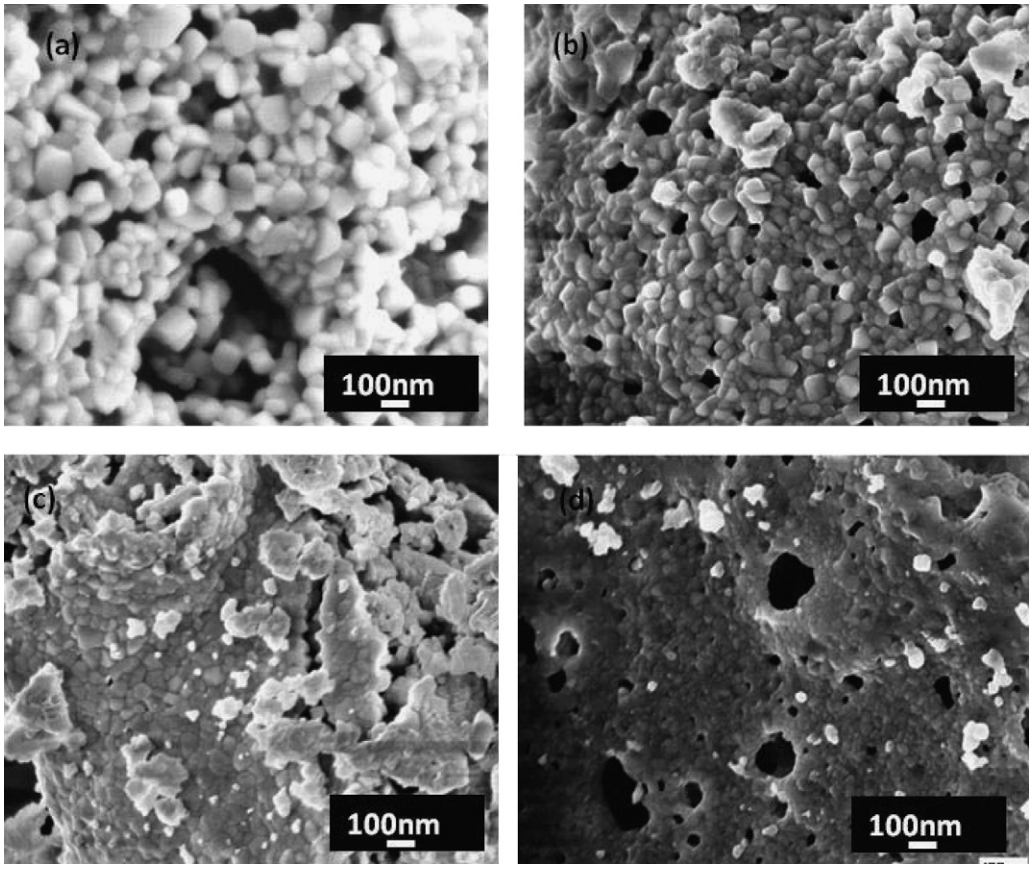

Fig. 4. SEM micrographs of (a) BNT, (b) 5 mol% Pr doping, (c) 10 mol% Pr doping and (d) 20 mol% Pr doping after calcination at 800 °C.

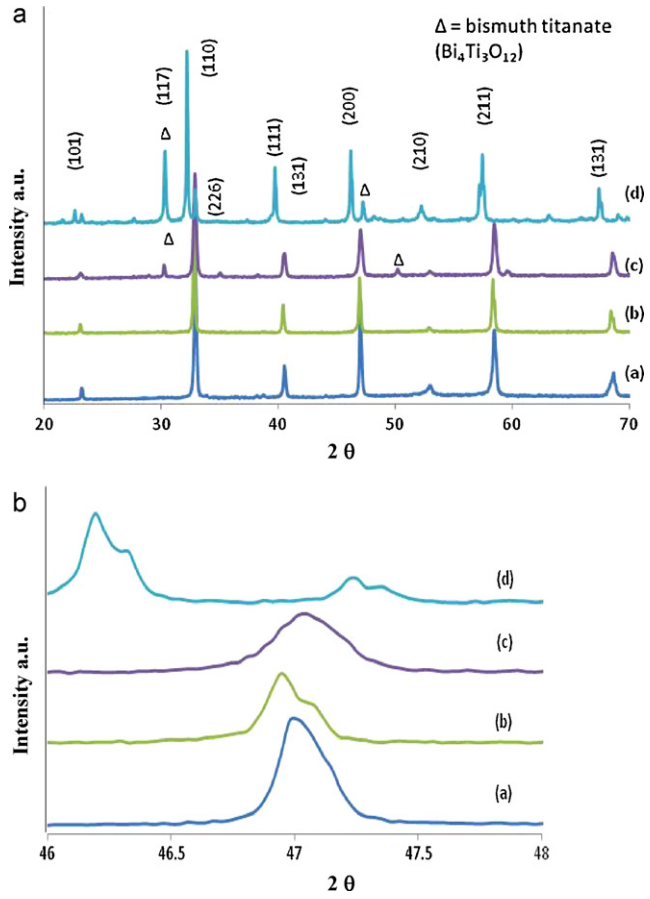

Fig. 5. XRD spectra of (a) BNT, (b) 5 mol% Pr doping, (c) 10 mol% Pr doping and (d) with 20 mol% Pr doping after sintering at 1100 °C. [a] Wide scan XRD spectra, [b] splitting of (*h* 0 *l*)- and (0 *k l*)-type reflections of (2 0 0) peak position.

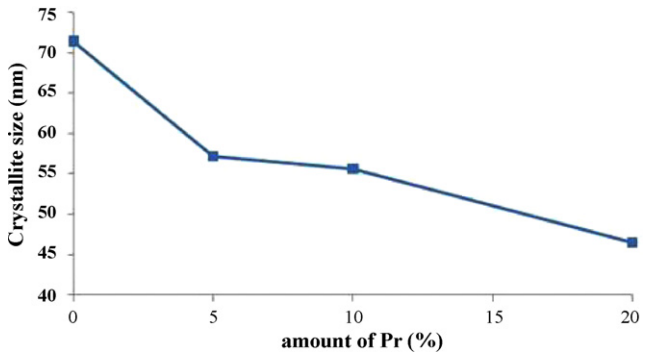

Fig. 6. Crystallite size of BNT and Pr-doped BNT after sintering at 1100 °C for 3 h.

doping of Pr to BNT. This micro-strain can be explained by Vegard's law, which suggests a linear relationship between the crystal lattice parameter and the concentration of the Pr dopant added. The increase of ion shift results in an increase of lattice energy to stabilize the structure. However, this increasing trend stopped at the 5 mol% level of Pr doping of BNT and started to shift to the right side with further addition of Pr. This result is in agreement with those of Lee et al. [16] and Liu et al. [14].

Fig. 2[b] shows that the intensity of the peak position (2 0 0) decreases with increasing concentration of Pr dopant. Pr-doped BNT was found to have a broader peak than that of undoped BNT, mainly because of compositional fluctuation or substitution disordering in the arrangement of cations at crystallographic sites in the lattice structure. Broadening of the peak indicates a decrease of crystallite size, which is confirmed by calculation using Scherrer's equation [$k = (0.9 \times \lambda)/(B \cos\theta)$], showing that crystallite size decreases with increasing amount of Pr, as shown in Fig. 3.

Fig. 4 shows the SEM micrographs of doped and undoped BNT after calcination at 800 °C. The grain size decreased gradually with increasing level of Pr doping. The SEM micrograph of undoped BNT shows the largest average grain size, around 215.86 nm. As levels of Pr dopant increased to 5, 10, 20 mol%, grain size decreased to 157.12 nm, 76.47 nm and 70.77 nm, respectively. In Pr-doped BNT, Pr acted as an inhibitor during the growth process. The slower diffusion rate of Pr ions than that of Bi ions caused Pr to inhibit the growth of grains [14].

The XRD spectra of BNT and Pr-doped BNT pellets sintered in air at 1100 °C for 3 h are shown in Fig. 5[a]. A single phase Pr-doped BNT was obtained up to the 5 mol% level of Pr doping (JCPDS No. 36-340). The secondary phase that was present in 10 mol% and 20 mol% Pr-doped BNT was bismuth titanate ($Bi_4Ti_3O_{12}$; BIT) (JCPDS No. 00-047-0398). When the amount of Pr dopant increased, the intensities of the BIT peaks became stronger, indicating that the secondary BIT phase became more dominant (with higher crystallinity) as the amount of dopant increased. When the amount of Pr dopant increased, more Pr^{3+} ions substituted Bi^{3+} ions, thus more bondless Bi^{3+} ions were available to react with Ti^{4+} and O^{2-} ions to form a greater amount of BIT phase.

Fig. 5[b] shows the XRD spectra of the splitting of (*h* 0 *l*)- and (0 *k l*) of BNT and Pr-doped BNT at $2\theta \sim 47^\circ$. BNT and BNT doped with Pr at $x = 0.10$ do not show any peak splitting caused by (*h* 0 *l*)- and (0 *k l*)-type reflections. Normally, splitting is caused by lattice distortion [20]. The peaks can be assigned to a (2 0 0/0 2 0) peak splitting following a rhombohedral symmetry and a tetragonal symmetry. The splitting shows that Pr doping tends to change the lattice parameter and distort the position of ions in the lattice. The result indicates the coexistence of rhombohedral and tetragonal phases, which is consistent with the nature of the specimen with its morphotropic phase boundary composition [21].

Fig. 6 shows the crystallite sizes of BNT with different levels of Pr doping after sintering at 1100 °C. In general, crystallite size of BNT increased after sintering, as it did in powder after calcination. For each composition, crystallite size decreased with increasing Pr doping in BNT. Crystallite size of undoped BNT was 71.4 nm whereas crystallite size of 5 mol% Pr-doped BNT was 57.2 nm. As the level of Pr doping in BNT increased to 10 mol% and 20 mol%, crystallite size continued to decrease, to 55.6 nm and 46.5 nm, respectively. Similarly, Watcharapasorn and Jiansirisomboon [7] have reported that dysprosium doped into BNT can cause grains of BNT to become smaller. McLaughlin [21] has reported that grain growth during sintering was suppressed with small levels of additives, but larger levels of additives increased grain size. However, this study found that BNT doped with Pr up to 20 mol% still suppressed crystallite size.

Fig. 7 shows SEM micrographs of BNT doped with different levels of Pr after sintering at 1100 °C for 3 h. The grain size of Pr-doped BNT was found to be clearly smaller than that of undoped BNT. Undoped BNT had a large grain size of greater than 10 μm whereas BNT at the 5 mol% level of Pr doping showed a much smaller grain size (683.152 nm). Pr appears to have acted as a grain growth inhibitor that influences the diffusion process during sintering. This finding is in agreement with that of Watcharapasorn and Jiansirisomboon [7]. By doping with a small amount of Pr, grain size can be reduced as the diffusivity of Pr becomes lower than that of Bi. Although grain size decreased with increasing Pr level, the highest density was obtained in 10 mol% Pr doping (Fig. 8). The result could be due to the closely packed structure of the grains at that level of doping.

The relative dielectric constant and loss tangent were measured at 25 °C with an electric field of 1 V, as shown in Fig. 9. BNT showed

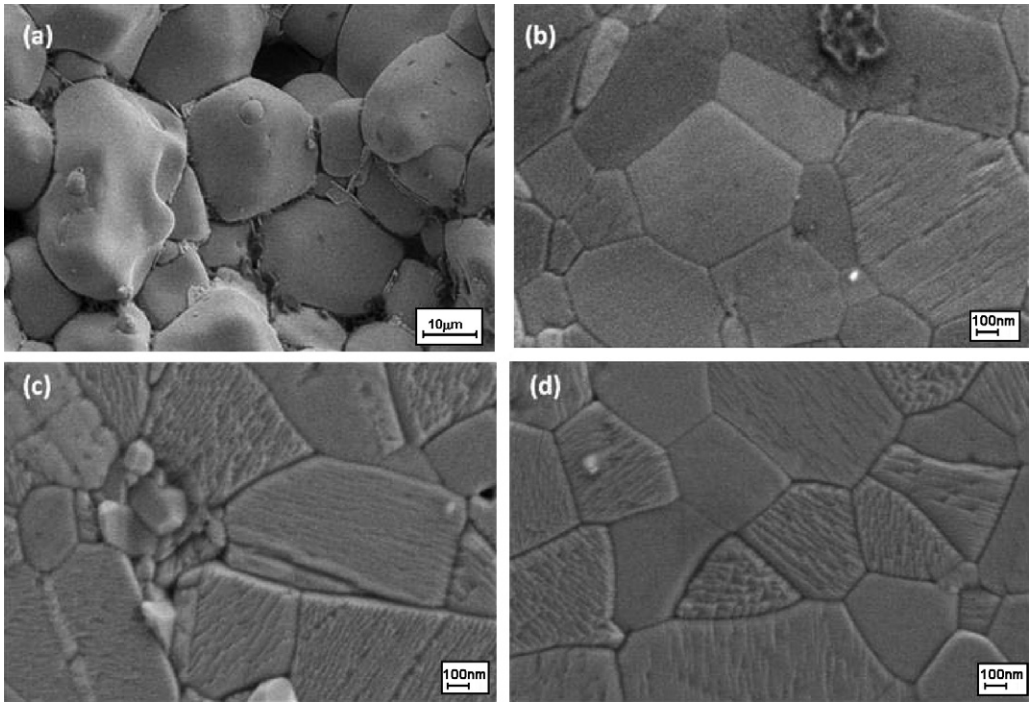

Fig. 7. SEM micrographs of (a) BNT, (b) 5 mol% Pr doping, (c) 10 mol% Pr doping and (d) 20 mol% Pr doping after sintering at 1100 °C for 3 h.

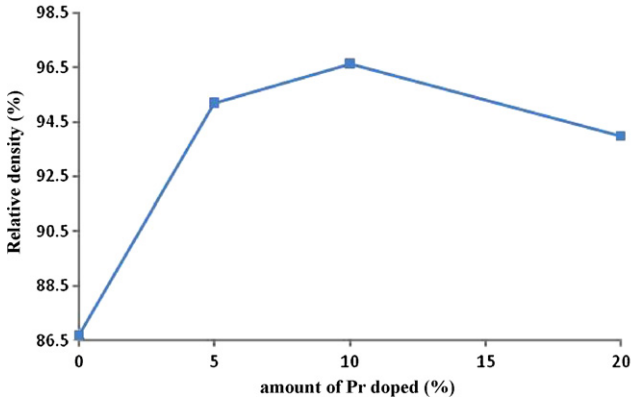

Fig. 8. Relative density of various amounts of Pr doped BNT after sintering at 1100 °C for 3 h.

the lowest dielectric constant value at only 347, whereas 5 mol% Pr-doped BNT had the highest dielectric constant value of 756. With Pr doping at a level higher than 5 mol%, the dielectric constant decreased. Pr-doped BNT improved the dielectric constant and reduced the loss tangent. The result could be explained by

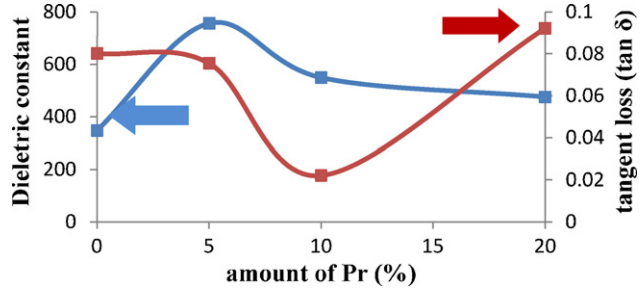

Fig. 9. Relative dielectric constant and loss tangent (tan δ) of (a) BNT, (b) 5 mol% Pr doping, (c) 10 mol% Pr doping and (d) 20 mol% Pr doping after sintering at 1100 °C for 3 h.

the presence of domains in the grains of the samples, influencing the dielectric properties. In BNT, large grains cause the presence of many 90° and 180° domains [19]. The presence of many domains in various directions suppressed the dielectric properties of the sample. At 5 mol% Pr doping, grain size was smaller than in BNT, causing lower domains presence in grains (Fig. 7). Therefore, dielectric properties of Pr-doped BNT were better than in BNT. However, further increase of Pr doping up to 20 mol% in BNT caused degradation of dielectric properties. This phenomenon was caused by the presence of stress in fine grains in ferroelectric region [19,22–25]. In large grains stress can be reduced by the arrangement of 90° domains. However, 90° domains are not present when grain size is fine. The absence of 90° domains in fine grains suppresses dielectric properties of whole samples due to the presence of unrelieved stress in the grains.

Pr doped BNT produced using soft combustion technique showed comparable dielectric constant value with other piezoelectric compounds such as $(K_{0.5}Na_{0.5})_{0.97}(Nb_{0.9}Ta_{0.1})O_3$ ($\varepsilon_r = 890$), $(PbMg_{1/3}Nb_{2/3})O_3$–$PbTiO_3$ ($\varepsilon_r = 797$) and $PbTiO_3$ ($\varepsilon_r = 200$) [26–28]. BNT produced in this work has lower dielectric constant compared to BNT produced using other techniques. The low dielectric constant value was caused by the small (submicron) grain size of the samples. In most research the grain size was larger than 5 μm [14,17,21]. The fine grains even after sintering could be beneficial in device miniaturization since the produced powders could be used as thick film instead of bulk pellets. Comparing with our previous work [12], BNT has a lower dielectric constant than that of BIT as a result of the substitution of Na for Bi. Up to 5 mol% Pr doped BNT enhanced the dielectric constant, but beyond that the dielectric constant decreased because Pr acted as grain growth inhibitor. On the other hand, the dielectric constant of Pr-doped BIT initially decreased up to 5 mol%, beyond which it increased. The result was due to increasing of grain size with increasing Pr doped BIT.

4. Conclusion

Pure BNT and Pr-doped BNT ceramic powders were successfully synthesized using the soft combustion technique after calcination

at 800 °C. However, after sintering at 1100 °C for 3 h, only 5 mol% Pr-doped BNT showed only a single phase while 10 and 20 mol% Pr-doped BNT showed the presence of secondary phase $Bi_4Ti_3O_{12}$. Grain size and crystallite size decreased with increasing Pr doping level because Pr acted at grain growth inhibitor. Optimum density was obtained with 10% Pr doping. The highest dielectric constant was obtained for 5 mol% Pr-doped BNT. The result could be due to the optimum grain size of the sample and the presence of a single phase in the compound.

Acknowledgments

The authors express sincere appreciation to the technical support of the School of Materials and Mineral Resources Engineering, Universiti Sains Malaysia. This research was supported by a Malaysian Research University grant 1001/PBahan/811069.

References

[1] X.P. Jiang, Y. Chen, K.H. Lam, S.H. Choy, J. Wang, J. Alloys Compd. 501 (2010) 323.
[2] D. Lin, K.W. Kwok, H.L.W. Chan, J. Alloys Compd. 461 (2008) 273.
[3] Q. Xu, M. Chen, W. Chen, H.-X. Liu, B.-H. Kim, B.-K. Ahn, J. Alloys Compd. 463 (2008) 275.
[4] L.F. Gao, Y.Q. Huang, Y. Hu, H.Y. Du, Ceram. Int. (2007) 1041.
[5] L. Huidong, F.F. Chude, Y. Wenlong, Mater. Lett. 58 (2004) 1194.
[6] X.X. Wang, K.W. Kwok, X.G. Tang, Solid State Commun. 129 (2004) 319.
[7] A. Watcharapasorn, S. Jiansirisomboon, Ceram. Int. 34 (2008) 769.
[8] Y. Hou, L. Hou, M. Zhu, H. Wang, H. Yan, Mater. Lett. 61 (2007) 3371.
[9] A. Ullah, C.W. Ahn, A. Hussain, I.W. Kim, Curr. Appl. Phys. 10 (2010) 1367.
[10] Y. Hou, B. Liu, L. Wei, Ceram. Int. 35 (2009) 1423.
[11] Y. Zhang, R. Chu, Z. Xu, J. Hao, Q. Chen, F. Peng, W. Li, G. Li, Q. Yin, J. Alloys Compd. 502 (2010) 341.
[12] P.Y. Goh, K.A. Razak, S. Sreekantan, J. Alloys Compd. 475 (2009) 758.
[13] M. Cernea, E. Andronescu, R. Radu, F. Fochi, C. Galassi, J. Alloys Compd. 490 (2009) 690.
[14] Y.F. Liu, Y.N. Lu, S.H. Dai, J. Alloys Compd. 484 (2009) 801.
[15] M. Raghavender, G.S. Kumar, G. Prasad, J. Phys. Chem. Solids 67 (2006) 1803.
[16] W.C. Lee, C.Y. Huang, L.K. Tsao, Y.C. Wu, J. Eur. Ceram. Soc. (2009) 1443.
[17] L. Ma, K. Zhao, J. Li, Q. Wu, M. Zhao, C. Wang, J. Rare Earth (2009) 496.
[18] E. Fukuchi, T. Kimura, J. Am. Ceram. Soc. (2002) 1461.
[19] N.N. Greenwood, A. Earnshaw, Chemistry of Elements, second ed., Butterworth Heinemann, 1998.
[20] Y.G. Wang, G. Xu, L.L. Yang, Z.H. Ren, X. Wei, W.J. Weng, P.Y. Du, G. Shen, G.R. Han, Ceram. Int. (2009) 1657.
[21] S.R. McLaughlin, PhD thesis, Queen's University Kingston, Ontario, 2008.
[22] C.R. Zhou, X.Y. Liu, Mater. Chem. Phys. (2008) 413.
[23] W. Cao, C.A. Randall, J. Phys. Chem. Solids 57 (1996) 1499.
[24] U. Helbig, J. Eur. Ceram. Soc. 27 (2007) 2567.
[25] M.-S. Yoon, N.H. Khansur, B.-K. Choi, Y.G. Lee, S.C. Ur, Ceram. Int. 35 (2009) 3027.
[26] D.W. Wua, R.M. Chen, Q.F. Zhou, K.K. Shung, D.M. Lin, H.L.W. Chan, Ultrasonics 49 (2009) 395.
[27] Q.F. Zhou, X.C. Xu, E.J. Gottlieb, L. Sun, J.M. Cannata, H. Ameri, M.S. Humayun, P.D. Han, K.K. Shung, IEEE Trans. Ultrason. Ferr. 54 (2007) 668–675.
[28] K.A. Snook, J.Z. Zhao, C.F. Alves, J.M. Cannata, W.H. Chen, R.J. Meyer, T.A. Ritter, K.K. Shung, IEEE Trans. Ultrason. Ferr. 49 (2002) 169.